

OROS: Orchestrating ROS-driven Collaborative Connected Robots in Mission-Critical Operations

Carmen Delgado*, Lanfranco Zanzi^{†‡}, Xi Li[†], Xavier Costa-Pérez^{*†§}

*i2CAT Foundation, Barcelona, Spain. Email:{name.surname}@i2cat.net

[†]NEC Laboratories Europe, Heidelberg, Germany, Email:{name.surname}@neclab.eu,

[‡] Technische Universität Kaiserslautern, Kaiserslautern, Germany

[§] ICREA, Barcelona, Spain.

Abstract—Battery life for collaborative robotics scenarios is a key challenge limiting operational uses and deployment in real life. Mission-Critical tasks are among the most relevant and challenging scenarios. As multiple and heterogeneous on-board sensors are required to explore unknown environments in simultaneous localization and mapping (SLAM) tasks, battery life problems are further exacerbated. Given the time-sensitivity of mission-critical operations, the successful completion of specific tasks in the minimum amount of time is of paramount importance. In this paper, we analyze the benefits of 5G-enabled collaborative robots by enhancing the Robot Operating System (ROS) capabilities with network orchestration features for energy-saving purposes. We propose *OROS*, a novel orchestration approach that minimizes mission-critical task completion times of 5G-connected robots by jointly optimizing robotic navigation and sensing together with infrastructure resources. Our results show that *OROS* significantly outperforms state-of-the-art solutions in exploration tasks completion times by exploiting 5G orchestration features for battery life extension.

Index Terms—5G, Orchestration, Robotics, Optimization

I. INTRODUCTION

Robots have been designed to interact with unknown environments and act on behalf of humans to minimize the risk of accidents or injuries. Thanks to their rapid deployment and relatively low cost, ground robots as well as Unmanned Aerial Vehicles (UAVs) have recently emerged as alternatives to address emergency and mission-critical scenarios [1] [2]. Such use-cases drive the evolution of simple remote-controlled robots into moving platforms equipped with dedicated operating systems, advanced computing capabilities and multiple communication modules, to support autonomous navigation and robot control tasks, which can be also aided by Artificial Intelligence (AI) based solutions to perform more accurate decisions thanks to real-time multi-sensor data streams.

However, a trade-off arises when pursuing higher degrees of robot autonomy. Moving robots require sufficient energy to operate in unknown environments throughout their mission. While mobility still represents the major cause of battery consumption [3], computing and processing of multi-sensor information are increasing their impact on available energy resources. At present, most of the real-world learning problems faced by robots can only be tackled by feeding dense data directly to more capable infrastructure and dedicated computing units [4]. Simultaneous localization and mapping (SLAM) and object recognition are only some example of robot applications

that may be needed during rescue operations and deployment of first-aid support [5]. Most of the modern solutions require the setup of dedicated local networks, e.g., WiFi-based, which limits the applicability of robot technology to only indoor environments [6].

In this context, the next generation of mobile networks (5G) is envisioned as a key-enabler to provide the outdoor wireless communication and enhance the autonomy of robotic applications [7]. The ubiquitous connectivity, high bandwidth and the low latency access provided by the modern mobile technologies, together with the possibility to seamlessly exploit multi-access edge computing platforms (MEC) deployed at the edge of the networks, and cloud computing to host processing and analytic services as virtual or container-based instances, would enable unprecedented levels of flexibility in the deployment of robotic applications which may efficiently off-load computing tasks to the edge and alleviate their energy consumption [8] [9].

In the 5G context, an orchestrating entity acts as a mediator in charge of guaranteeing the most efficient use of the infrastructure resources, while pursuing the satisfaction of heterogeneous communication requirements. Similarly, an orchestration entity can be adopted in the robot domain to control the multitude of operational modules and sensors installed on the on-board robot platform, e.g., to optimize energy consumption and resource utilization. However, in the state-of-the-art both orchestration entities work independently, with little to no awareness of each other during the operational phases. On the one hand, the robot domain assumes ubiquitous and unlimited resource availability, both from the networking and cloud resource perspective, which leads to performance drops when dealing with wireless and virtualized environments, especially in heterogeneous multi-robot scenarios. On the other hand, the 5G domain operates without knowledge of the actual resource requirements from the robot domain, mainly by over-provisioning the resources. This introduces inefficient networking resource usage and, perhaps more importantly, waste of energy in the robots, making it hard for such energy-constrained devices to fulfill their tasks.

To fill this gap, in this work we propose to combine the orchestration logic from the network infrastructure and the robot domains, enabling information exchange between the robots and the hosting infrastructure. In this way, not only

energy-aware decisions performed in the robotic domain may be tuned according to real-time infrastructure conditions, but also infrastructure resources can be re-configured to meet robot communication and energy requirements in a dynamic and efficient manner. The main contributions of this paper include:

- We propose an optimization approach combining the orchestration of the 5G mobile infrastructure including mobile edge jointly with the energy-aware optimization of the on-board robot sensor applications.
- We design a framework for the deployment of robotic applications with the 5G infrastructure, defining the interfaces and the interactions between the proposed joint orchestration logic with the individual robot orchestrator and the 5G orchestrator.
- We evaluate our proposed approach by means of an exhaustive simulation campaign, showcasing the achievable gains deriving from the joint orchestration of the 5G infrastructure and robot applications, both in terms of exploration time as well as the resulting energy savings.

The remainder of the paper is structured as follows. Section II summarizes related works in the field. Section III presents the main building blocks of our architecture and describes the interaction among the different modules. Section IV formulates our optimization problem detailing our model assumptions. Section V validates the design principles of our solution by means of a comprehensive simulation campaign highlighting the main benefits deriving from our approach. Finally, Section VI concludes this paper.

II. RELATED WORK

Several works in the literature investigate the adoption of mobile networks to control robots in outdoor scenarios. In [10] the authors propose a framework for the offloading of time-critical and computational exhaustive operations onto a distributed node architecture, where the communication between the robot and the cloud server is done via 5G.

Despite offloading computational intensive task would help robots to save energy, in realistic environments the limited energy availability provided by on-board batteries still represents a major limitation. Ideally, robots would require the largest batteries in order to extend their mobility range. At the same time, heavier batteries would impact on their energy consumption rate, thus introducing a design trade-off [11].

Swanborn *et al.* identify robot navigation as the main energy consumer [3] at runtime. Additionally, they identify secondary sources of energy consumption, such as inefficient hardware, inefficient management algorithms, idle times, operational inefficiencies (e.g., poor quality software that leads to unnecessary stops and/or turns, as well as sharp acceleration and deceleration), processing energy, and finally, unnecessary communication and wasting of sensor data acquisition. We highlight that our solution will positively affect the last two drawbacks.

To optimize the exploration of unknown areas, several energy-aware management schemes have been proposed in the literature. [12] proposes an approach for energy efficient path

planning during autonomous mobile robot exploration. The idea is for a unique robot to efficiently explore the environment and periodically return to the starting point of the exploration for recharging its battery. The periodicity depends on an adaptive threshold that concurrently considers the movement of the robot, its power consumption and the current state of the environment. The authors focus on minimizing the overall travel path in order to minimize the energy consumption. Since exploring an area poses hard limits in a single robot settings, in their follow up work they extended the idea to teams of coordinated robots sharing a limited number of Charging Points (CPs) while exploring a structured, unknown environment with unknown obstacles. The objective in this case aims at exploring the area as fast as possible [13]. Since it is infeasible to pre-compute an optimized schedule due to a limited time horizon, an energy-aware planner is used for adaptive decision making on when and where to recharge. However, their results are limited to numerical simulations.

Similarly, Benkrid *et al.* investigate the problem of multi-robot exploration in unknown environments. In their work, they propose a decentralized coordination approach to minimize the exploration time while considering the total motion energy saving of the mobile robots [14]. The exploration target is defined as a segment of the environment including the frontiers between the unknown and the explored areas. Each robot evaluates its relative rank, and compare it with the other robots of the team considering the energy consumption to reach this exploration target. As a result, the robot is assigned to the segment for which it has the lowest rank. They evaluate their proposal through simulation experiments as well as ROS-enabled robots. However, inaccuracies during the robot localization and the map generation are not considered. Additionally, they only consider scenarios with unlimited energy availability, or limited energy without the possibility of recharging.

Nevertheless, none of the above works considers networking aspects in their optimization, nor adopt an NFV approach for their deployments. Recent works such as [15] and [16], started exploring the benefits of adopting 5G and cloud-native deployment in robotic applications exploiting the offloading of computational tasks to fog, edge or cloud systems so as to build a cloud-to-things continuum. Despite their promising results, the current research is mainly focusing on virtualization aspects, and on the development of orchestration platforms to automate the deployment and allocation of both networking and computing resources over the 5G infrastructure. However, such orchestration platforms only control the infrastructure resources, and neither consider the internal logic of robotic applications nor decide any actions for the robots. To the best of our knowledge, this is the first work to jointly consider robots and infrastructure resource orchestration, pursuing robot energy consumption optimization.

III. FRAMEWORK OVERVIEW

As depicted in Fig. 1, we consider a set of ground robots deployed in an unknown outdoor environment, where wireless

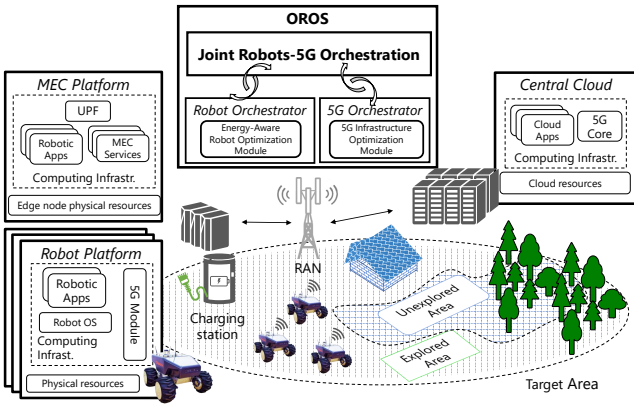


Fig. 1. Overview of the architectural building blocks.

communication is provided by means of a 5G network. We assume a 5G Radio Access Network (RAN) composed by a set of base stations (gNBs) providing radio coverage over the area of interest. We also assume the presence of an edge and a remote cloud platforms, to host robotic applications and the 5G core functionalities, respectively, running as virtual or container-based instances within a computing infrastructure. A non-exhaustive list of robot applications include motion planning, video processing, etc., while the 5G core accounts for the set of user authentication, connection setup and mobility management functionalities proper of a mobile network. We assume the robot controller running in the edge premises, and rely on the presence of a User Plane Function (UPF) to seamlessly route the 5G data plane traffic generated by the robots to the edge platform, therefore favouring low-latency communication and wider bandwidth availability.

In this work, we focus on a surveillance (public protection and disaster relief) use-case. Cloud-based robots can perform 24/7 security inspections, replacing security personnel, reducing cost and storing all data needed. They collect video and images and send them to the cloud for real-time identification of suspicious people and activity. Similar robots are already being used at airports and in outdoor rescue scenarios [17].

A. Robot Orchestration

In this paper we build on the Robot Operating System (ROS) design and specifications [18] for the control and orchestration of robots and the onboarding of robotic applications. ROS is an open-source robotics middleware that provides common functionality (e.g., read sensor data, navigation, planning, etc.) over general hardware abstraction using low-level device control. It contains a collection of tools, libraries, APIs and conventions that simplify the task of creating complex and robust robot behaviour across a variety of robotic systems [19].

A system built using ROS consists of a number of processes, potentially on a number of different hosts, connected at runtime in a peer-to-peer topology. The ROS topology is supported by a lookup mechanism to allow processes to find each other in real time. The mechanism is implemented through ROS Masters and ROS nodes. While a ROS Master

represents a stateless entity that coordinates the ROS nodes, the ROS nodes communicate with each other by passing messages, which are defined with a strictly typed data structure and published through topics. ROS was initially designed for standalone robotic applications, with the centralized design for serving a single robot in a local area network. As such, it is not suitable in upcoming multi-robot cloud-based applications, which demand for a distributed environment containing a variety of networking and cloud resources to be concurrently coordinated in order to connect and control multiple robots in potentially distributed areas.

In its latest releases [20], ROS mitigates the issue of real-time topic sharing over a distributed platform by means of a novel Data Distributed Service (DDS), while supporting more flexible container-based deployments [21]. In order to seamlessly control robots and related robotic applications, we envision the *Robot Orchestrator* entity as composed by a layered architecture consisting of three layers: application layer, ROS client layer, and ROS middleware layer. The application layer hosts a variety of robotic applications offered with run-time application programming capabilities. The ROS client layer provides a set of ROS client APIs [22] based on the built-in ROS client libraries to the developer interface supporting different languages such as C, C++, Python. The ROS middleware layer offers a set of APIs [23] to enable compatibility with different interchangeable low-level communication protocols, and support distributed data and service sharing. Through these provided APIs, the robot orchestrator is able to translate the application logic into a set of instructions to control and coordinate groups of robots via ROS command messages dispatched through its Southbound Interface (SBI).

B. 5G Orchestration

In its simplest definition, a 5G Orchestrator is in charge of the allocation and management of the 5G infrastructure resources, including those required to enable robots communication and transmit their application data, as well as the set of computing resources to host and run the robotic control plane applications. For example, a 5G orchestration solution may decide on the amount of radio resources to be allocated in order to support both the robot control plane (e.g., navigation and velocity commands), and the robot data plane (e.g., video and sensor data) communications. Besides, the robot applications can be deployed in a virtualized environment, e.g., being containerized in a local or a cloud computing infrastructure. In such case, the 5G orchestrator is also in charge of the life-cycle management of such container-based robotic application instances, including their on-boarding, instantiation and termination, automatic scaling and self-healing operations. At last but not least, the 5G orchestrator can also determine a proper placement strategy of placing robotic applications which, thanks to softwarealized and cloud-native approaches, may be deployed locally, i.e., onto the robot computing infrastructure, or remotely, in edge and cloud platforms, or even adopting hybrid approaches. Nevertheless, an accurate placement strategy demands for

proactive resource allocation in order to decide optimal amount of computing, memory and storage resources to support the provisioning of various robotic applications, both onto the robots and edge/cloud platforms. The 5G orchestrator can be built relying on existing open source orchestrator platforms such as Open Source MANO (OSM) or leveraging on open-source orchestration platforms developed for instance in [24] [25]. From a system architecture perspective, the 5G orchestrator consists of three layers: service layer, orchestration layer and resource layer. The service layer defines an *intent engine* to receive and process the application requests, translating the application requirements and mapping them to *network slices* in the form of network slice template as defined by the 3GPP TS 28.531 [26] and the network slice resource model (3GPP TS 28.541 [27]). The orchestration layer consists of a *Management and Network Orchestration (MANO)* stack to enforce the OROS 5G policy on the allocation of resources, placement and life-cycle management of the robotic applications. These include the instantiation and releasing of computing resources to host drivers and processing instances managing the corresponding sensors on the robots, and their associated applications on a computing infrastructure when activating or deactivating sensors. On the bottom is the resource layer. It includes a *Virtual Infrastructure Manager (VIM)*, which interacts with the underlying physical infrastructure and offers unified abstractions over the heterogeneous set of mobile resources. It carries out monitoring, allocation and management of resources across the infrastructure and exposes this information to the orchestrator engine to guide its tasks.

C. OROS

So far, major effort has been taken in the definition of orchestrating platforms in each corresponding domain, e.g., OSM [28], ONAP [29] in the 5G domain, and ROS [18] in the robotic environment. However, the orchestration tasks work independently, and lack of dedicated data models and interfaces to interconnect them. Traditionally, robot navigation and path planning processing are performed by a local robot controller deployed within the same premises. When considering modern smart multi-robot platforms instead, a dedicated controller entity is generally located in the cloud. On the one hand, to enable the communication from the central controller entity to the individual robots, mobile network resources should be allocated and also adapted to guarantee the bandwidth and latency requirements, especially when computing offloading is also part of the robot task. On the other hand, enabled by the NFV technologies, modern robot sensing devices not only produce (and/or consume) sensor data, but also can be controlled by dedicated software applications (e.g., based on ROS) running on top of a shared computing infrastructure. Without a joint orchestration solution, these software instances will always remain active and consume the infrastructure resources, impacting on the overall energy consumption. In this scenario, we advocate for the adoption of novel application-oriented orchestration solutions to guide the overall life-cycle management of cloud computing resources, provisioning of

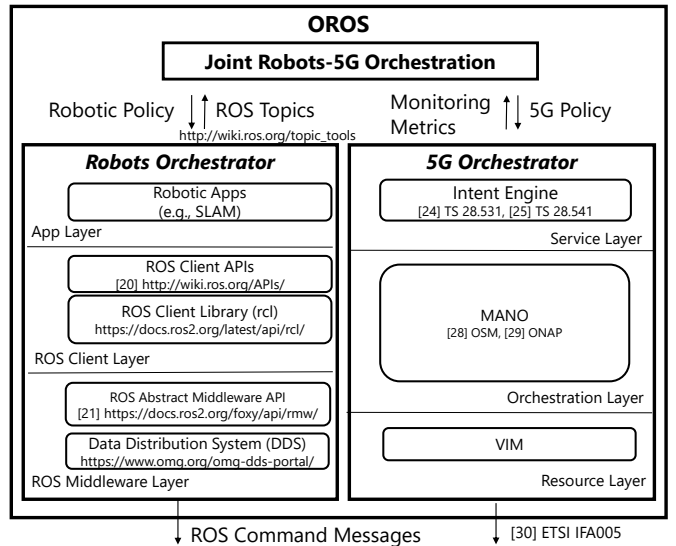


Fig. 2. Architecture overview of the OROS solution.

dedicated resources, and context-aware robot motion planning, pursuing energy savings strategies. To fill this gap, in this work we propose OROS, a solution for the joint orchestration of the robotic and 5G ecosystem, to control ROS-driven collaborative connected robots in 5G networks. The architecture design of the proposed OROS solution is depicted in Fig. 2. OROS seamlessly connects the orchestrating entities of the two domains, and coordinates their operations via a joint Robots-5G Orchestration module, as the central brain of our solution.

During the operation phase, assuming that the robotic applications are already instantiated and running, the joint Robots-5G orchestration module makes high-level joint orchestration decisions, namely *Robotic Policies* and *5G Policies*, and sends to each domain-specific orchestrator. It relies on the input taken from the monitoring metrics exposed by the Robot Orchestrator via its Northbound Interface (NBI) (e.g., ROS topics detailing velocity, location, and power consumption of the robots), and those exposed by the 5G Orchestrator (e.g., radio resource availability, and computing resources on the MEC and robot platforms for running the robotic applications, etc.). Upon receiving the robotic policy, the Robot Orchestrator is in charge of reconfiguring the related robotic applications and translating the required corresponding actions to robot command messages, through exploiting the provided ROS client and middleware APIs. Examples of these include instructing the robot to move towards its new navigation goal, or switch off a specific sensor to save the energy. In the 5G domain, once receiving a new 5G policy from the joint optimization module, the Intent Engine will translate the received policy to update the corresponding network slices based on the new requirements. The 5G orchestration engine will further process the slice update request and optimize the reallocation of 5G resources (e.g., RAN, core, and MEC). This includes the instantiation and release of the networking and computing resources associated to the robotic applications, which can

be switched on/off depending on the decision of OROS. Moreover, the 5G orchestration decides on the migration of the robotic applications towards the MEC and robot platforms. These decisions will be forwarded to the MANO to execute the operation workflows, and consequently to the VIM in order to enforce the configurations of the resources on the robot platforms and the 5G infrastructure via the SBI following ETSI IFA 005 specifications [30]. In the following Section IV, we detail the energy-aware mathematical formulation that guides the orchestration decisions while interacting with the specific domain orchestrators.

IV. PROBLEM FORMULATION

A. OROS - Joint Robots-5G Orchestration Optimization

Hereafter, we present our assumptions, notation and problem formulation to address the Energy-Aware Optimization problem. All variables and system parameters are resumed in Table I to allow faster referencing.

Input variables Let us consider a discrete set of time instants denoted by the set $\mathcal{T} = \{t_1, \dots, t_{|\mathcal{T}|}\}$, and a set of robot devices $\mathcal{R} = \{r_1, \dots, r_{|\mathcal{R}|}\}$. Each robot $r \in \mathcal{R}$ is equipped with a rechargeable battery characterized by a limited capacity B_{max} , $\forall r \in \mathcal{R}$, whose charging status $b_{r,t}$ varies over time depending on the robot operational activities, i.e., $0 \leq b_{r,t} \leq B_{max}$, $\forall t \in \mathcal{T}$. Each robot is also equipped with multiple sensors, such as cameras, lidar, etc.

We assume robots to be deployed in an outdoor environment covered by a mobile infrastructure, as to enable 5G connectivity. Without loss of generality, let us define the area of interest with dimensions $A \times B$ meters, and decompose the 2D surface into a grid $\mathcal{G} = \{g_{a,b}, \forall (a,b) \in (A,B)\}$, where each element $g_{a,b} \in \mathcal{G}$ needs to be explored by at least one robot during the operational phase. The dimension of $g_{a,b}$, i.e., $|g_{a,b}|$, depends on the maximum field of view of the adopted robot camera and sensors, and we assume such cameras/sensors to be able to provide a 360° view of the surrounding environment.

Each robot needs to receive periodical updates from the radio interface, as well as upload sensed environmental information. For doing so, each robot adapts the Modulation and Coding Schemes (MCS) used according to the perceived channel quality, which we assume proportional to the instantaneous distance of the robot to the serving base station, as will be later detailed in Section V. We assume the serving base station located at position $(g_{BS,b_{BS}}) \in \mathcal{G}$.

To keep track of the multi-robot exploration, we introduce $e_{t,a,b}$ as a binary variable indicating if the 2D area unit $g_{a,b}$ has been already explored at time t , or not. Exploration of unknown areas may require charging stations to extend the operational time of rescue robots. We assume the presence of a charging station (CS) located in position $(g_{CS,b_{CS}}) \in \mathcal{G}$, which is known a-priori to all robots, and that can be either available or unavailable (due to an already charging robot) at a certain time instant. The CS provides a charging rate CR to recover the robot battery level.

We define Δt as the period between two instants in \mathcal{T} (i.e., $\Delta t = |t_t - t_{t-1}|$), and assume the spatial mobility of every

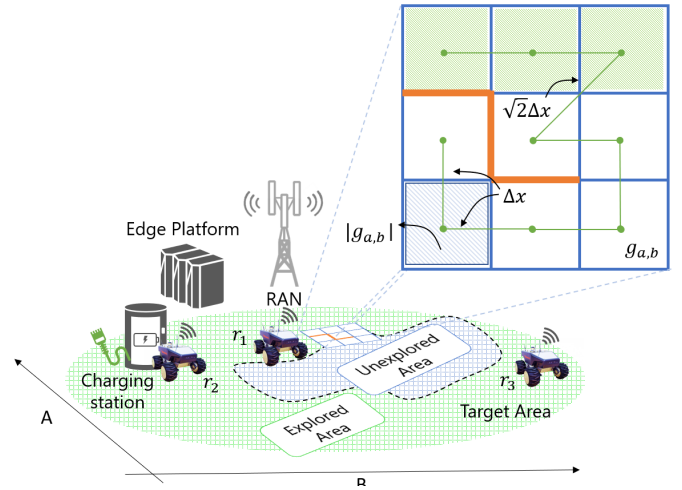


Fig. 3. Example of the robot exploration problem solved with multiple robots.

robot $r \in \mathcal{R}$ limited to a unit of distance Δx for every Δt , where Δx is the distance between the centers of two neighbour area units $g_{a,b}$ and $g_{a',b'}$ as depicted in Fig. 3. Therefore, it turns that each robot moves at a velocity $\frac{\Delta x}{\Delta t}$ if moving into the left/right or up/down directions, but moves at velocity $\frac{\sqrt{2}\Delta x}{\Delta t}$ when travelling in diagonal directions. Clearly, if the velocity increases, so does the corresponding energy cost. We consider this by introducing the terrain-velocity constant $m_{a,b,a',b'}$ $\forall a,a' \in A, \forall b,b' \in B$, which weights the energy consumption of the robots from moving from position $g_{a,b}$ to position $g_{a',b'}$. The value of $m_{a,b,a',b'}$ is set to infinite in presence of an obstacle, therefore influencing its mobility in the corresponding unit of area. Whenever the robot moves, we can derive its power consumption by adapting Equation 1 of Rappaport [12], where instead of only computing the velocity, we consider the terrain-velocity constant to account for obstacles and terrain conformity form as:

$$P_{move_{a,b,a',b'}} = 0.29 + 7.4m_{a,b,a',b'}. \quad (1)$$

As mentioned before, robots exploit an existing mobile infrastructure to communicate with the orchestrating entity. We introduce $P_{TX,a,b}$ as a variable representing the energy consumed by the robot for transmitting data. The actual robot transmit power should be adapted as to compensate the radio path-loss. Therefore, the value of $P_{TX,a,b}$ depends on the current robot location $(g_{a,b})$ and its distance from the serving base station. Similarly, robots consume energy for receiving data. In this case, we introduce P_{RX} as a constant value independent of the robot location. Finally, since robots need to map and explore the terrain, they need to use their camera and sensors, as well as process those data to avoid inefficient raw data transmission. We collect the energy consumption derived by all these activities in the variable P_{SEN} , which represents the energy consumed by robot sensors and corresponding local data processing. We assume this variable also to include the energy consumption coming from the computing infrastructure locally running on the robot.

TABLE I
MODEL PARAMETERS

Parameter	Definition
$\mathcal{T} = \{t_1, \dots, t_{ \mathcal{T} }\}$	Set of time instants; index t refers to time instant t_t
$\mathcal{R} = \{r_1, \dots, r_{ \mathcal{R} }\}$	Set of robots; index r refers to task r_r
$A \times B$	Geometric dimensions of the area of interest
$\mathcal{G} = \{g_{a,b}, \forall (a,b) \in (A,B)\}$	Grid representing the area to be explored
$m_{a,b,a',b'}$	Terrain-velocity constant for moving from position $g_{a,b}$ to $g_{a',b'}$
$u_{r,t}$	Binary decision variable indicating if the charging station is being used at time t by robot r
$l_{r,t,a,b}$	Binary decision variable indicating if robot r is in position $g_{a,b}$ at time instant t
$e_{t,a,b}$	Binary variable indicating if the unit of area $g_{a,b}$ has been explored at time t
$b_{r,t}$	Continuous variable indicating the battery level of robot r at time instant t , where $0 \leq b_{r,t} \leq B_{max}$
CR	Charging rate provided by the charging station
$P_{move_{a,b,a',b'}}$	Power consumed by moving from position $g_{a,b}$ to position $g_{a',b'}$
P_{RX}	Power consumed for receiving a packet
$P_{TX,a,b}$	Power consumed for transmitting a packet
P_{SEN}	Power consumed by activating sensors, local data processing and computing infrastructure

Decision variables Let $l_{r,t,a,b}$ be a binary decision variable to control the robot mobility. Its value gets positive if the robot r is at position $g_{a,b}$ at time instant t . Similarly, we introduce $u_{r,t}$ as a binary decision variable performing decisions on which robot r has to recharge its battery at time t .

Objective To explore an unknown area as fast as possible, and therefore increase the chances of detecting the target object (or person), we need to maximize the explored area within the given time period $|\mathcal{T}| \times \Delta t$, therefore we can write our objective function as:

$$\max \sum_{t \in \mathcal{T}} \sum_{(a,b) \in (A,B)} e_{t,a,b} \quad (2)$$

Constraints We assume that the charging station can only recharge one robot $r \in \mathcal{R}$ at every time instant $t \in \mathcal{T}$, therefore we introduce the following constraint:

$$\sum_{r \in \mathcal{R}} u_{r,t} \leq 1 \quad \forall t \in \mathcal{T}, \quad (3)$$

additionally, a robot $r \in \mathcal{R}$ can be charged at some time $t \in \mathcal{T}$ only if the robot is in the charging station at that specific time instant t :

$$u_{r,t} \leq l_{r,t,a_{CS},b_{CS}} \quad \forall t \in \mathcal{T}, \forall r \in \mathcal{R}. \quad (4)$$

Clearly, the duration of the recharge period may comprise multiple time intervals t , to allow more energy to fill the battery. With the following constraint, we ensure that each robot $r \in \mathcal{R}$ can only be in one place in every time instant $t \in \mathcal{T}$:

$$\sum_{(a,b) \in (A,B)} l_{r,t,a,b} = 1 \quad \forall r \in \mathcal{R}, \forall t \in \mathcal{T}. \quad (5)$$

In order to keep track of the exploration progress among multiple robots, if any robot $r \in \mathcal{R}$ visited an area unit $g_{a,b} \in (A,B)$ at some earlier time, or if it is exploring such area unit at the current time t , that area becomes explored at time t and we update the variable $e_{t,a,b}$ accordingly:

$$e_{t,a,b} \leq e_{t-1,a,b} + \sum_{r \in \mathcal{R}} l_{r,t,a,b} \quad \forall t \in \mathcal{T}, \forall (a,b) \in (A,B), \quad (6)$$

$$e_{t,a,b} \geq e_{t-1,a,b} \quad \forall t \in \mathcal{T}, \forall (a,b) \in (A,B), \quad (7)$$

$$|\mathcal{R}| e_{t,a,b} \geq \sum_{r \in \mathcal{R}} l_{r,t,a,b} \quad \forall t \in \mathcal{T}, \forall (a,b) \in (A,B). \quad (8)$$

With the following constraint we define the mobility boundaries of the robots, and ensure that for each Δt a robot $r \in \mathcal{R}$ can only move to a neighbour area unit, or stay in the same position:

$$\begin{aligned} l_{r,t+1,a,b} &\leq l_{r,t,a,b} + l_{r,t,a-1,b} + l_{r,t,a+1,b} + l_{r,t,a,b-1} + \\ &l_{r,t,a,b+1} + l_{r,t,a-1,b-1} + l_{r,t,a+1,b+1} + l_{r,t,a-1,b+1} + \\ &l_{r,t,a+1,b-1} \quad \forall r \in \mathcal{R}, \forall t \in \mathcal{T}, \forall (a,b) \in (A,B). \end{aligned} \quad (9)$$

Equation 9 affects the robot velocity. In fact, as mentioned before, the velocity and therefore the power consumption depends on the direction of the robot movement. This is taken into account in the constant $P_{move_{a,b,a',b'}}$. Conversely, if the robot is at the charging station and it is being charged (i.e., $u_{r,t} = 1$), the energy level of its battery increases with a constant charging rate CR . Furthermore, in every time instant the robot is not charging, it sends or receives data. When transmitting, the consumed power depends on the distance to the base station (according to $P_{TX,a,b}$), while in case of reception it depends on P_{RX} as previously discussed. Finally, if a robot has never been in an area unit, its sensors, camera, processing units and transmission elements should be active. However, if the robot is in an already explored area, an advanced orchestration solution may turn them off for saving energy. Robots are expected to be reachable by the managing entity in every time instant. For this reason, we assume robots never switch off their receiving antennas. Taking this into account, the battery level $b_{r,t}$ gets updated in every time instant by the following equation:

$$\begin{aligned} b_{r,t+1} &= b_{r,t} + CR \times u_{r,t+1} - P_{RX} \times (1 - u_{r,t+1}) - \\ &\sum_{(a,b) \in (A,B)} \sum_{(a',b') \in (A,B)} l_{r,t,a,b} \times l_{r,t+1,a',b'} \times P_{move_{a,b,a',b'}} \\ &- P_{SEN} \times \sum_{(a,b) \in (A,B)} (1 - e_{t,a,b}) \times l_{r,t+1,a,b} - \\ &\sum_{(a,b) \in (A,B)} P_{TX,a,b} \times (1 - e_{t,a,b}) \times l_{r,t,a,b} \quad \forall t \in \mathcal{T}, \forall r \in \mathcal{R}. \end{aligned} \quad (10)$$

B. Energy-Aware SLAM Comparison Benchmark

In order to compare our energy-aware algorithm, we introduce a benchmark that does not allow to dynamically turn off the robot sensors, even if robots are travelling within an already explored area. This means that whenever the robot is not charging, its camera and processing units are enabled, and sensor data is flowing through the closest base station. To ensure fair comparison, we maintain the same objective function (see Equation 2), as well as the same set of constraints, whereas we replace Equation 10 to enforce the energy-aware SLAM scenario as the following:

$$\begin{aligned}
 b_{r,t+1} = & b_{r,t} + CR \times u_{r,t+1} - (P_{RX} + P_{SEN}) \times (1 - u_{r,t+1}) \\
 & - \sum_{(a,b) \in (A,B)} \sum_{(a',b') \in (A,B)} l_{r,t,a,b} \times l_{r,t+1,a',b'} \times P_{move_{a,b,a',b'}} \\
 & - \sum_{(a,b) \in (A,B)} P_{TX,a,b} \times (1 - u_{r,t+1}) \times l_{r,t+1,a,b} \\
 & \forall t \in \mathcal{T}, \forall r \in \mathcal{R}.
 \end{aligned} \tag{11}$$

Finally, we can introduce our benchmark scenario as:

Problem SLAM:

$$\max \sum_{t \in \mathcal{T}} \sum_{(a,b) \in (A,B)} e_{t,a,b}$$

subject to:

$$(3)(4)(5)(6)(7)(8)(9)(11);$$

We highlight that this approach is also energy-aware, meaning that it allows robots to follow the best path to explore the area as fast as possible, taking into account the available energy on the battery, and the possibility of recharging it.

V. PERFORMANCE EVALUATION

In this section, we evaluate the performance of the energy-aware optimization module when dealing with collaborative robot scenarios. We first introduce the scenario setup. Then, in order to evaluate the orchestration benefit, we compare our OROS energy-aware optimization module that is capable of managing the sensing applications (as seen in Section IV-A), against the standard SLAM approach, which does not allow to dynamically turn on and off the sensing modules when robots are in already explored areas (see Section IV-B).

A. Scenario Setup and Methodology

In our evaluation, we consider a variable set of robots that need to be jointly orchestrated as to explore an unknown area in the fastest possible way. Table II resumes the experimental parameters used in our evaluation.

All robots start their exploration from the same point within the area of interest, co-located with the charging station. We set $\Delta t = 10s$ and $\Delta x = 10m$, which translates into $|g_{a,b}| = 100m^2$. This allows to derive the velocity of the robot as $\frac{\Delta x}{\Delta t} = 1m/s$ if it moves into the up/down/left/right direction, or at $\frac{\sqrt{2}\Delta x}{\Delta t} = \sqrt{2}m/s$ when moving in diagonal, which is in line with the maximum speed of $2m/s$ provided by commercial robot devices [31]. Each robot is equipped with a

TABLE II
EXPERIMENTAL SETUP

Definition	Value	Definition	Value
$ \mathcal{T} $	15	$ \mathcal{R} $	1,2,3
$A \times B$	$40 \times 40 m^2$	$ g_{a,b} $	$10 \times 10 m^2$
B_{max}	5000 J	Δt	10 s
CR	9.24 J/s	v	1, $\sqrt{2}$ m/s
$TxPower$	20 dBm	$ReceiverGain$	-20 dB
$PowerNoise$	-104 dBm	P_{RX}	4 W
P_{SEN}	12 W		

fully charged battery at the beginning of the exploration phase. About the charging station, in our experiment we consider the worst case scenario with a single charging station providing the lowest charging rate among the possible commercial options, i.e., $CR = 9.24J/s$, as in the case of TurtleBot3¹. We characterize the energy consumed by the robot for locomotion, sensor operation and radio wireless communication as follows. First, the power consumed by the locomotion $P_{move_{a,b,a',b'}}$ (see Equation 1) depends on the terrain-velocity constant $m_{a,b,a',b'}$, which also takes into account detected obstacles. This constant can be defined as:

$$m_{a,b,a',b'} = \begin{cases} 0 & \text{if } a' = a \text{ and } b' = b \\ \infty & \text{if there is an obstacle} \\ & \text{between } (a,b) \text{ and } (a',b') \\ v = \{1, \sqrt{2}\} & \text{if } a' \neq a \text{ or } b' \neq b \end{cases} \tag{12}$$

where v is the velocity in m/s. Note that we assume no power consumption for turning the robot in the desired direction. Second, we characterize the power consumed by the sensors P_{SEN} , which includes processing all the generated data by the camera, lidar and other sensors, as well as the power consumed by the local computing infrastructure. Based on the values from [32], we set it to take a value of $12W$.

Finally, we consider each robot is equipped with a 5G New Radio (NR) antenna module consuming energy whenever transmitting or receiving data. The power dissipated by the robot depends on its distance from the serving base station and on the corresponding Signal to Noise Ratio (SNR) which, in turn, affects the adoption of a particular MCS. The processing power consumed to encode radio packets is also affected by the instantaneous MCS in use. A detailed characterization of the power consumption in virtual base station as function of the MCS can be obtained from [33]. In our evaluation we set a transmission power of 20 dBm, a receiver gain of $-20dB$, a Power Noise of $-104dBm$ and a carrier frequency of $3.5GHz$, as determined by 3GPP [34]. In case of downlink transmission, we consider an average value of $4W$ according to the measurements of [33], and assume the receiving module always on, to enable reachability of the robot devices with control messages at any time. We use the Gurobi solver [35] to address the optimization problem described in Section IV.

¹<https://www.robotis.us/lipo-battery-charger-lbc-010/>

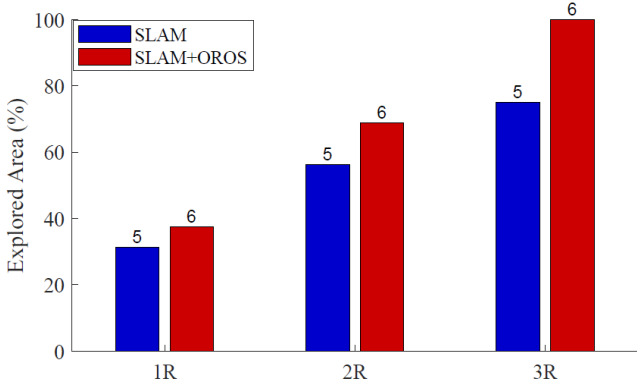


Fig. 4. Area Explored when robots do not charge.

B. Assessing the gain of the orchestrator

Hereafter we compare our OROS against the SLAM approach. As our work targets mission-critical use-cases, we advocate for the adoption of the area exploration rate as main metric of interest. This would allow to compare different approaches, and identify the one that maximises such objective in the shortest time. Starting from an obstacle-free scenario of $40 \times 40 m^2$, Fig. 4 depicts the resulting discovery performances for the two approaches when deploying an increasing number of robots, namely 1, 2 or 3. For each strategy, we detail at the top of each bar the time spent (in epoch) to reach the corresponding explored area. In this first example we do not consider the presence of a recharging station, however when using 3 robots we are able to explore the full area within the time boundaries. It is straightforward to understand that the concurrent deployment of multiple robots allows to explore additional areas in the same amount of time. Therefore, in order to focus the attention on our main findings, in this work we do not consider the adoption of an extreme number of robot devices. In particular, in the worst case scenario, i.e. when only a single robot is deployed (and there is no option to recharge), it can only explore the 31.25% of the area when not using OROS, while reaching a rate of 37.5% with our solution, highlighting the effects of a more efficient battery usage. Such improvement gets even more evident when considering an increasing number of robots. In the two robots scenario for example, we move the overall exploration rate from 56.25% to 68.75%, at the cost of 1 additional time epoch. Finally, when 3 robots are simultaneously active in the target area, the benefit of our approach is maximized, moving the ratio of explored area from 75% to 100%, while also using 1 additional time epoch as in the previous case.

Fig. 5 depicts the overall evolution of the exploration rate over time, for each of the two approaches and for an increasing number of robots. After an initial exploration phase, whose rate linearly grows with the number of rescue devices deployed in the field, robots need to follow their path back to the charging station. This, together with the amount of time to recharge the batteries leads to a non-increasing exploration rate. In the 1 robot - SLAM scenario this is particularly evident. After recharging, the robot restarts its exploration task

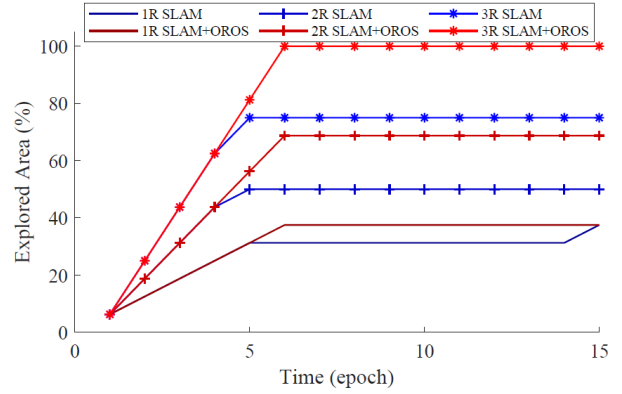


Fig. 5. Explored Area over time when one robot is able to charge.

which translates into the exploration rate growth during the 15-th epoch. Obviously, this time may be shortened by employing more recharge stations, or making use of a faster charging rate.

C. Sensitivity Analysis

In the following, we perform a sensitivity analysis on several key-parameters of our model formulation assessing the impact of their variation onto the overall system performances.

First, we evaluate the influence of different sensing power consumption, dubbed as P_{SEN} in our formulation, due to increasing or decreasing computation requirements, e.g., local video processing, or novel robot sensors. In particular, Fig. 6 displays the achieved explored area by two rescue robots when the power consumed by the sensors and by the underlying robot computing infrastructure varies, e.g., due to larger volume of traffic or intense processing. In this case, additionally to the reference value of 12W resumed in Table II, we consider both less-demanding scenarios and two extremely energy binding scenarios. From the picture, we can appreciate the influence of P_{SEN} on the robot exploration performances and how, in general, the exploration rate is reduced for an increasing sensor power consumption value. Interestingly, the gap between the SLAM approach and our proposed OROS follows an opposite trend. This is due to the fact that our smart orchestration allows turning off the sensors when the robot is in an area that has already been explored, therefore limiting the overall energy consumption. Despite the higher exploration gap is achieved in the worst case scenario $P_{SEN} = 36W$, we also notice how extreme sensor energy requirements actually affect the overall robot mobility, finally leading to fully discharged batteries within a shorter number of time epochs, e.g., 4 and 5 for the SLAM and OROS approaches, respectively.

Conversely, in Fig. 7 we analyze the robot performances for a variable battery capacity, namely B_{max} . We remark that its value affects the battery level of the rescue robots, as we assume them to start their task in a fully-charged state. As before, we consider a two robot scenario and the reference value reported in Table II (i.e., 5000J), as well as additional testing values accounting for greater (i.e., 10000J and 20000J) and more constrained capacities (i.e., 2500J and 1250J). If we

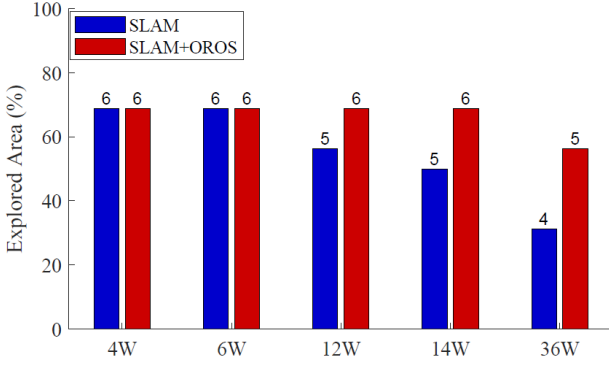


Fig. 6. Explored Area for variable P_{SEN} values.

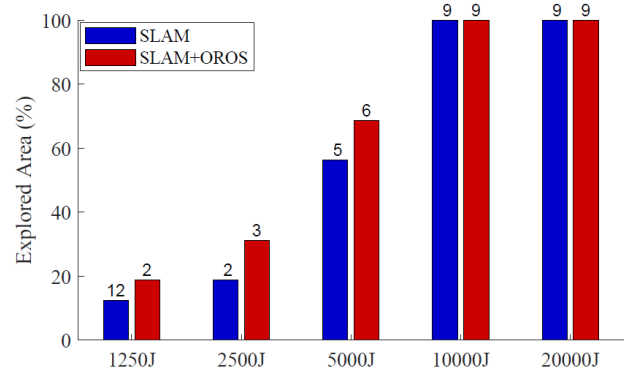


Fig. 7. Explored Area for variable B_{max} values.

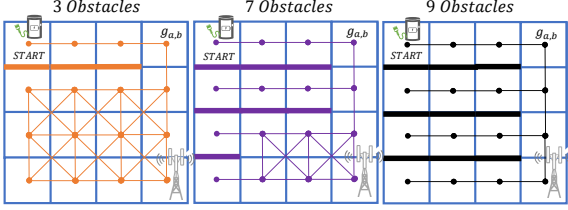


Fig. 8. Example of robot navigation paths for 3, 7 and 9 obstacles.

provide the robots with an energy reserve greater than 10000J, 2 robots are enough to completely explore the area of interest within the time boundaries. In this case, the impact of a smart resource orchestration over the exploration rate is negligible. Nevertheless, OROS allows maintaining a higher charge level in the robot's batteries at the end of the run. In particular, for the 10000J case when OROS is in place robots end with 1784.88J and 2051.76J respectively, while their remaining energy is 1445.88J and 1882.26J when adopting the SLAM approach. On the other side, despite the presence of a recharge station, if we decrease the battery capacity we limit the robot mobility and reduce the achievable exploration rate. Robots can explore less than a third of the overall area of interest (exactly 31.25%) with limited 2500J batteries. In case of 1250J, this further reduces to 18.75% in 2 epochs when using OROS, while without it, robots are capable of exploring only 12.5% of the space, thus needing 12 epochs.

D. Area with obstacles

In the previous subsections, we considered barrier-free scenarios and focus our study on the sensitivity analysis. Hereafter, we consider a more realistic scenario and introduce not surmountable obstacles along the robot path, and evaluate the overall system performances with constrained robot mobility.

Obstacles are introduced as horizontal lines at the edge of two adjacent grid elements, and they are placed as to avoid unreachable sub-areas. For the sake of visualization, in Fig. 8 we consider a small-scale scenario and depict all possible robot navigation paths for an increasing number of obstacles, namely 3, 7 and 9. For the 3 obstacles, the number of possible movements is actually much higher than when there are 9 obstacles. Fig. 9 builds on the scenario depicted in Fig. 8, and summarizes the explored area in presence of obstacles,

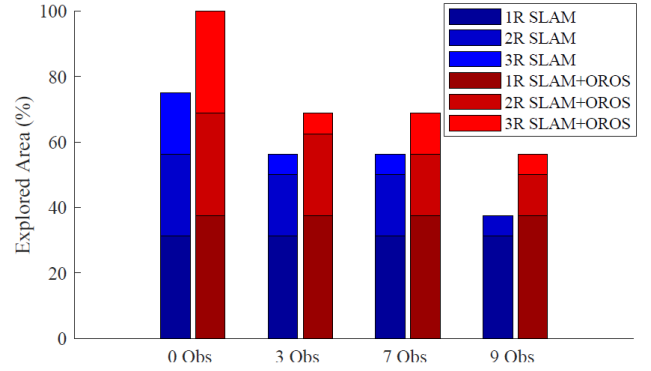


Fig. 9. Effects of an increasing number of obstacles.

comparing the performances for an increasing number of collaborative robots and the two discussed approaches. To ease the comparison, each bar provides an incremental view with respect to the reference scenario with a larger number of robots. For example, in absence of obstacles, by adopting 3 robots at the end of the experiment about 20% more of the target area was explored when compared with the 2 robots scenario. It can be noticed how performances remain constant when a single robot is adopted into the research task. This is in line with our previous results considering the limited energy availability (5000J): an increasing number of obstacles has no impact due to a poor mobility range.

Conversely, in multi-robot scenarios, obstacles limit the available paths and induce lower exploration rates. In particular, due to the special geometry of our scenario, obstacles are mostly affecting the initial exploration phase, leading the different robots to follow the same path in their initial steps. When increasing to the maximum number of robots, either 3 or 7 obstacles have the same impact on performances, while in case of 9 obstacles, the achievable exploration rate is highly reduced. Interestingly, in this case using 3 or 2 robots provides the same performances due to the constrained navigation paths when using the SLAM approach, while OROS outperforms the benchmark in all the considered tests, confirming that the adoption of a smart orchestration solution provides significant benefits in collaborative exploration scenarios.

VI. CONCLUSIONS

Due to limited computing and energy resource availability, cloud-based robot deployments rely on mobile infrastructure to enable collective robotic intelligence exchange and increase their efficiency when performing tasks. However, current solutions are limited by the fact that robot operating systems and ICT computing and communication platforms, do not have means to interact with each other. In this paper, we propose a joint optimization framework for the concurrent orchestration of the robotic, computing and communication infrastructure domains. Our results show that mission-critical collaborative robot operations would benefit from the adoption of OROS, a joint orchestration solution which significantly improves tasks completion duration by reducing overall energy consumption. Future work will focus on the implementation of the proposed OROS framework in real deployments, comprising off-the-shelf outdoor robots and 5G commercial infrastructure.

ACKNOWLEDGMENT

The research leading to these results has been supported by the Spanish Ministry of Economic Affairs and Digital Transformation and the European Union - NextGeneration EU (project no. TSI-063000-2021-6), by the CERCA Programme from the Generalitat de Catalunya, and by the European Union's H2020 5G ERA Project (grant no. 101016681).

REFERENCES

- [1] A. Albanese, V. Sciancalepore, and X. Costa-Pérez, "SARDO: An Automated Search-and-Rescue Drone-based Solution for Victims Localization," *IEEE Transactions on Mobile Computing*, pp. 1–1, 2021.
- [2] R. Fantacci, F. Gei, D. Marabissi, and L. Micciullo, "Public safety networks evolution toward broadband: sharing infrastructures and spectrum with commercial systems," *IEEE Communications Magazine*, vol. 54, no. 4, pp. 24–30, Apr. 2016.
- [3] S. Swanborn and I. Malavolta, "Energy Efficiency in Robotics Software: A Systematic Literature Review," *IEEE/ACM International Conference on Automated Software Engineering Workshops*, pp. 144–151, 2020.
- [4] L. Ferranti, S. D'Oro, L. Bonati, E. Demirors, F. Cuomo, and T. Melodia, "HIRO-NET: Self-Organized Robotic Mesh Networking for Internet Sharing in Disaster Scenarios," in *IEEE WoWMoM*, 2019, pp. 1–9.
- [5] S. Saedi, M. Trentini, M. Seto, and H. Li, "Multiple-Robot Simultaneous Localization and Mapping: A Review," *Journal of Field Robotics*, vol. 33, no. 1, p. 3746, Jan. 2016.
- [6] C. Cadena, L. Carlone, H. Carrillo, Y. Latif, D. Scaramuzza, J. Neira, I. Reid, and J. J. Leonard, "Past, Present, and Future of Simultaneous Localization and Mapping: Toward the Robust-Perception Age," *IEEE Transactions on Robotics*, vol. 32, no. 6, pp. 1309–1332, Dec. 2016.
- [7] M. Aleksy, F. Dai, N. Enayati, P. Rost, and G. Pocovi, "Utilizing 5G in Industrial Robotic Applications," in *International Conference on Future Internet of Things and Cloud (FiCloud)*, Aug. 2019, pp. 278–284.
- [8] P. Skarin, W. Tärneberg, K.-E. Arzen, and M. Kihl, "Towards Mission-Critical Control at the Edge and Over 5G," in *IEEE International Conference on Edge Computing (EDGE)*, Sept. 2018, pp. 50–57.
- [9] V. Petrov, M. A. Lema, M. Gapeyenko, K. Antonakoglou, D. Moltchanov, F. Sardis, A. Samuylov, S. Andreev, Y. Koucheryavy, and M. Dohler, "Achieving End-to-End Reliability of Mission-Critical Traffic in Softwarized 5G Networks," *IEEE Journal on Selected Areas in Communications*, vol. 36, no. 3, pp. 485–501, Mar. 2018.
- [10] F. Voigtländer, A. Ramadan, J. Eichinger, C. Lenz, D. Pensky, and A. Knoll, "5G for robotics: Ultra-low latency control of distributed robotic systems," *International Symposium on Computer Science and Intelligent Controls (ISCSIC)*, pp. 69–72, 2017.
- [11] M. Albonico, I. Malavolta, G. Pinto, E. Guzman, K. Chinnappan, and P. Lago, "Mining Energy-Related Practices in Robotics Software," in *Mining Software Repositories Conference (MSR)*, May 2021.
- [12] M. Rappaport, "Energy-aware mobile robot exploration with adaptive decision thresholds," *International Symposium on Robotics (ISR)*, pp. 236–243, 2016.
- [13] M. Rappaport and C. Bettstetter, "Coordinated recharging of mobile robots during exploration," *IEEE International Conference on Intelligent Robots and Systems*, vol. 2017-Septe, pp. 6809–6816, 2017.
- [14] A. Benkrird, A. Benallegue, and N. Achour, "Multi-robot Coordination for Energy-Efficient Exploration," *Journal of Control, Automation and Electrical Systems*, vol. 30, no. 6, pp. 911–920, 2019.
- [15] C. Guimarães, M. Groshev, L. Cominardi, A. Zabala, L. M. Contreras, S. T. Talat, C. Zhang, S. Hazra, A. Mourad, and A. de la Oliva, "Deep: A vertical-oriented intelligent and automated platform for the edge and fog," *IEEE Communications Magazine*, vol. 59, no. 6, pp. 66–72, 2021.
- [16] L. Girletti, M. Groshev, C. Guimarães, C. J. Bernardos, and A. de la Oliva, "An intelligent edge-based digital twin for robotics," in *2020 IEEE Globecom Workshops*, 2020, pp. 1–6.
- [17] Z. Gui and H. Li, "Automated Defect Detection and Visualization for the Robotic Airport Runway Inspection," *IEEE Access*, vol. 8, pp. 76 100–76 107, May 2020.
- [18] Stanford Artificial Intelligence Laboratory et al., "Robot Operating System," 2021 (accessed June 2021). [Online]. Available: <https://www.ros.org/>
- [19] M. Quigley, K. Conley, B. P. Gerkey, J. Faust, T. Foote, J. Leibs, R. Wheeler, and A. Y. Ng, "ROS: an open-source Robot Operating System," in *ICRA Workshop on Open Source Software*, 2009.
- [20] Y. Maruyama, S. Kato, and T. Azumi, "Exploring the Performance of ROS2," in *International Conference on Embedded Software*, 2016.
- [21] S. Aldegheri, N. Bombieri, F. Fummi, S. Girardi, R. Muradore, and N. Piccinelli, "Enabling Containerized Computing and Orchestration of ROS-Based Robotic SW Applications on Cloud-Server-Edge Architectures: Late Breaking Results," in *ACM/EDAC/IEEE Design Automation Conference*, 2020.
- [22] ROS Wiki, "ROS wiki APIs," 2021 (accessed July 2021). [Online]. Available: <http://wiki.ros.org/APIs/>
- [23] ROS2, "ROS Middleware Abstraction Interface ," 2021 (accessed July 2021). [Online]. Available: <https://docs.ros2.org/foxy/api/rmw/>
- [24] X. Li et al., "Automating Vertical Services Deployments over the 5GT Platform," *IEEE Communications Magazine*, vol. 58, no. 7, pp. 44 – 50, July 2020.
- [25] X. Li, A. Garcia-Saavedra, X. Perez, C. Bernardos, C. Guimaraes, K. Antevski, J. Mangués, J. Baranda, E. Zeydan, D. Corujo, P. Iovanna, G. Landi, J. Alonso, P. Paixao, H. Martins, M. Lorenzo, J. Ordoñez-Lucena, and D. López, "5Growth: An End-to-End Service Platform for Automated Deployment and Management of Vertical Services over 5G Networks," *IEEE Communications Magazine*, vol. 59, no. 3, pp. 84–90, March 2021.
- [26] 3GPP (Third Generation Partnership Project), "Management and orchestration; Provisioning, TS 28.531, V15.4.0," Sep. 2019.
- [27] —, "Management and orchestration; 5G Network Resource Model (NRM), TS 28.541, V16.3.0," Dec. 2019.
- [28] ETSI, "Open source MANO (OSM) project," 2021 (accessed June 2021). [Online]. Available: <https://www.osm.etsi.org/>
- [29] L. Foundation, "Open Network Automation Platform," 2021 (accessed June 2021). [Online]. Available: <https://www.onap.org/>
- [30] ETSI, "ETSI GS NFV-IFA 005 v2.1.1, Network Function Virtualisation (NFV); Management and Orchestration; Or-Vi reference point ? Interface and Information Model Specification," 2016.
- [31] N. Seegmiller and D. Wettergreen, "Optical Flow Odometry with Robustness to Self-shadowing," in *IEEE International Conference on Intelligent Robots and Systems*, Sept. 2011, pp. 613–618.
- [32] Y. Mei, Y. H. Lu, Y. C. Hu, and C. S. Lee, "A case study of mobile robot's energy consumption and conservation techniques," *International Conference on Advanced Robotics (ICAR)*, pp. 492–497, Jul. 2005.
- [33] J. A. Ayala-Romero, I. Khalid, A. Garcia-Saavedra, X. Costa-Perez, and G. Iosifidis, "Experimental evaluation of power consumption in virtualized base stations," in *IEEE International Conference on Communications (ICC)*, Jun. 2021.
- [34] 3GPP (Third Generation Partnership Project), "Technical Specification Group Radio Access Network; Study on channel model for frequencies from 0.5 to 100 GHz," in *Technical Report*, 2017.
- [35] Gurobi Optimization, LLC, "Gurobi Optimizer Reference Manual," 2021. [Online]. Available: <https://www.gurobi.com>